

# High-pressure Induced Conformational and Phase Transformations of 1,2-Dichloroethane Probed by Raman Spectroscopy

Robert J. Sabharwal, Yining Huang, and Yang Song\*

Department of Chemistry, The University of Western Ontario, London, Ontario N6A 5B7, Canada

Received: December 2, 2006; In Final Form: March 19, 2007

1,2-Dichloroethane (DCE) was loaded into diamond anvil cells and compressed up to 30 GPa at room temperature. Pressure-induced transformations were probed using Raman spectroscopy. At pressures below 0.6 GPa, fluid DCE exists in two conformations, gauche and trans in equilibrium, which is shifted to gauche on compression. DCE transforms to a solid phase with exclusive trans conformation upon further compression. All the characteristic Raman shifts remain constant in fluid phase and move to higher frequencies in the solid phase with increasing pressure. At about 4–5 GPa, DCE transforms from a possible disordered phase into a crystalline phase as evidenced by the observation of several lattice modes and peak narrowing. At 8–9 GPa, dramatic changes in Raman patterns of DCE were observed. The splitting of the C–C–Cl bending mode at  $325\text{ cm}^{-1}$ , together with the observation of inactive internal mode at  $684\text{ cm}^{-1}$  as well as new lattice modes indicates another pressure-induced phase transformation. All Raman modes exhibit significant changes in pressure dependence at the transformation pressure. The new phase remains crystalline, but likely with a lower symmetry. The observed transformations are reversible in the entire pressure region upon decompression.

## I. Introduction

Pressure-induced phase transitions, chemical reactions as well as formation of novel structures have received increasing attention.<sup>1,2</sup> As one of the fundamental thermodynamic parameters, pressure plays a significant role in regulating the total energies of highly compressible molecular solids by changing the inter- and intramolecular distances. At elevated pressures, structural and chemical stabilities can be completely altered and thus a wide variety of transformations are often induced. Among these transformations, pressure mediated conformational equilibrium is of particular interest because the reactivity of many organic reagents, product yields, and even reaction pathways are strongly correlated with molecular conformations. Halogen substituted ethane on the two carbon atoms represent a class of simplest organic molecules that exhibit conformational information, i.e., trans versus gauche, depending on the relative orientations of the halogens attached to the two carbons. A model molecule, 1,2-dichloroethane (DCE), the two conformations of which are shown in Figure 1, for example, has been studied extensively at ambient conditions and low-pressure regime by various means including vibrational spectroscopy and X-ray diffraction.<sup>3–9</sup> With recent advances in the static high-pressure technique and associated characterization probes, such molecules can be now studied far beyond the P–T region previously accessible.<sup>10</sup> Diamond anvil cells (DAC) have been widely used as a fundamental apparatus to achieve static high pressures in a broad temperature range. Vibrational spectroscopy, including Raman and Fourier transform infrared (FTIR) spectroscopy, provides sensitive probes for in situ structural characterization of materials loaded into DAC.<sup>2,11–13</sup>

Conformational study of DCE has been well documented at ambient conditions both experimentally and theoretically.<sup>3,4,8</sup> In gaseous and fluid phases, DCE exists as a mixture of trans

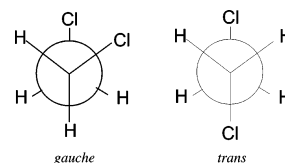


Figure 1. Newman projections of two conformers of DCE.

and gauche conformers with respective  $C_{2h}$  and  $C_2$  symmetry, but only as trans conformer in the solid phase. Out of a total of 18 vibrational modes for trans conformer, 9 modes ( $6A_g + 3B_g$ ) are Raman active and 9 modes ( $4A_u + 5B_u$ ) IR active, while all modes are both Raman and IR active for gauche conformer.<sup>3</sup> The active Raman and IR modes for DCE in different phases exhibit different characteristic frequencies and have been unambiguously assigned.<sup>4</sup> Therefore, Raman and IR spectroscopy can be used for quantitative conformational analysis on DCE. For instance, IR measurements together with ab initio calculations reported by Georgieva et al.<sup>8</sup> indicates that gaseous DCE is composed of 80% trans and 20% gauche conformers.

DCE has also been studied under pressures using vibrational spectroscopy previously. For example, the Whalley group reported a series of studies of pressure effects on conformational equilibrium of DCE in different solvents with different concentrations.<sup>5–7</sup> Taniguchi et al.<sup>6</sup> reported a Raman study of DCE in n-hexane solutions at pressures up to 0.5 GPa at room temperature. The ratio of integrated intensities of characteristic C–Cl stretching modes of gauche- versus trans-DCE was monitored as a function of pressure. The gauche population is found to increase with pressure associated with a negative change of conformational volume. Quantitative analysis of the volume change established the contributions from the change of Cl–C–C–Cl dihedral angle, molecular packing efficiency, as well as volume change of the solvent. More recently, McClain et al.<sup>14</sup> conducted a quantitative thermodynamic analysis of DCE

\* Corresponding author. E-mail: yang.song@uwo.ca. Phone: (519)661-2111 ext. 86310. Fax: (519)661-3022.

**TABLE 1: Summary of High-Pressure Studies of 1,2-Dichloroethane**

method	P–T range	conditions	phases	ref
Raman	0.5 GPa, room-T	in hexane and other solvent	trans, gauche	Taniguchi, et al. <sup>6</sup>
Raman, IR	1.5 GPa, room-T	in hexane solvent	trans, gauche	Takaya et al. <sup>5</sup>
Raman	2.5 GPa, 298–373 K	in diethyl ether solvent	trans, gauche	McClain et al. <sup>14</sup>
IR	3.6 GPa, room-T	in 2-methylbutane solvent	trans, gauche	Ikawa, et al. <sup>7</sup>
X-ray Diffraction	1.5 GPa, 177 and 280 K	single-crystal in situ	$\alpha$ - $\beta$ -phases, a new polymorph	Bujak et al. <sup>9</sup>
Raman	30 GPa, room-T	pure substance	trans, gauche, three solid phases	this work

in diethyl ether solution at different temperatures and pressures up to 2.5 GPa. Beyond that pressure, Ikawa et al.<sup>7</sup> loaded DCE into a DAC with 2-methylbutane as solvent. The system was compressed up to 3.6 GPa at room temperature and probed by IR spectroscopy. In the low-pressure range (<0.5 GPa), trans–gauche transformation was monitored by the relative IR intensities of the C–Cl stretching mode. The pressure effect on the transformation was found consistent with previous Raman measurement even in a different solution. However, in the pressure range of 0.5–3 GPa, the relative population of the trans and gauche conformers remains constant. With different concentrations of DCE in 2-methylbutane, trans–gauche equilibrium exhibits almost identical response to pressure, all reaching a maximum gauche/trans ratio at 0.5 GPa. This suggests that Cl–C–C–Cl dihedral angle of DCE decreases with pressure only below 0.5 GPa, but remains fairly constant above that pressure. Instead, the Cl–C–C angle increases due to the Cl–Cl repulsion at constant dihedral angle with increasing pressure.

In addition to vibrational spectroscopy, the structures of DCE were also characterized by extensive X-ray diffraction measurements. The Lipscomb group reported the first crystal structure of DCE using single-crystal diffraction at 223 K and near ambient pressures (0.1 MPa).<sup>15</sup> Later on, the same group reported another low-temperature phase at 133 K<sup>16</sup>, the structure of which was re-determined by Boese et al.<sup>17</sup> at a similar temperature of 110 K. As mentioned, DCE takes the trans conformation exclusively in solid phase below its melting point at 238 K at ambient pressure. The two observed solid phases were documented as disordered high-temperature  $\alpha$ -phase and ordered low-temperature  $\beta$ -phase. The  $\alpha \rightarrow \beta$  transformation temperature was determined to be 177 K at ambient pressure. Both phases are monoclinic with space group of  $P2_1/c$  and slightly different unit cell parameters, but both with two molecules per unit cell. More recently, Bujak et al.<sup>9</sup> reported an X-ray diffraction study of single-crystal DCE high pressures and room temperature where the structures of DCE are refined and a new pressure-induced polymorph was observed.

Despite the numerous previous studies of structures of DCE, the spectroscopic study has only been conducted in solutions, and all previous studies are limited in the low-pressure region (<4 GPa) as summarized in Table 1. In the low-pressure region, pressure effect on pure DCE should be of particular interest in terms of the relative population of the two conformers. In high-pressure region beyond 4 GPa, pressure effect on the structures of DCE remains completely unknown. In this study, we take the advantage of DAC techniques with Raman microspectroscopic probe to investigate the structures and transformations of DCE in the pressure region up to 30 GPa, far beyond the previously achievable pressures. New phases of solid DCE can be unambiguously identified from Raman patterns by analysis of pressure evolution of vibrational frequencies as well as the band profiles. The possible structures of the new phases are studied in combination with previous X-ray diffraction measurement. Finally, the reversibility of the transformations was examined by decompression. These new observations contribute

to the understanding of high-pressure structures of solid DCE and thus provide useful information of its stability, reactivity and other important thermodynamic properties.

## II. Experimental

Pure 1,2-dichloroethane (99%) was purchased from Aldrich and used without further purification. Two types of DAC were used. A P-type lever-arm DAC from High-pressure Diamond Optics Inc. equipped with type I diamonds with culet size of 650  $\mu\text{m}$  was used in the low-pressure region. With this DAC, predrilled stainless steel gaskets with a hole of diameter of 250  $\mu\text{m}$  were used for the study up to 4 GPa. This type of DAC allows accurate control of pressure and fine increments in the low-pressure region. Another symmetric piston-cylinder type of DAC equipped with 400  $\mu\text{m}$  culet diamond anvils was used to achieve pressures up to 30 GPa. A few ruby ( $\text{Cr}^{+3}$  doped  $\alpha\text{-Al}_2\text{O}_3$ ) chips as pressure calibrant were carefully placed inside the gasket sample chamber before the sample was loaded. The pressure was determined from the well-known pressure shift of the  $R_1$  ruby fluorescence line (at 694.2 nm under ambient conditions) with an accuracy of  $\pm 0.05$  GPa under quasi-hydrostatic conditions.<sup>18</sup> For the entire pressure region, ruby fluorescence spectra obtained on different ruby chips across the sample chamber indicate no significant pressure gradient and the spectral profile suggests good hydrostatic behavior, especially in the low-pressure region (e.g., <0.6 GPa).

A commercial Renishaw Raman spectrometer (Model 2000) was used for pressure determination and Raman measurements. This model is a compact laser Raman microprobe capable of both spectroscopy and imaging. A HeNe laser (632.8 nm) was used as the excitation source with average power of several milliwatts on the sample. A Leica microscope with objective lenses of multiple magnifications together with other Raman optics enables measurements in a back-scattering geometry. An edge filter is installed to remove the Rayleigh and anti-Stokes lines enabling a measurable spectral range above 120  $\text{cm}^{-1}$ . The spectrometer is further equipped with an imaging spectrograph and a sensitive thermoelectronically cooled CCD detector allowing a spectral resolution of 1  $\text{cm}^{-1}$ . Spectral calibration of the Raman spectrum was realized using silicon and diamond standards achieving an accuracy of  $\pm 0.5$   $\text{cm}^{-1}$ . Due to the strong  $T_{2g}$  mode of the type I diamond Raman signal at 1334  $\text{cm}^{-1}$ , the spectra were collected in the ranges of 100–1300 and 2600–3200  $\text{cm}^{-1}$ . These spectral ranges covered almost all the Raman active modes of DCE, except the  $\text{CH}_2$  wagging mode ( $\nu_{16}$  at 1318  $\text{cm}^{-1}$ ) and a  $\text{CH}_2$  bending mode ( $\nu_2$  at 1454  $\text{cm}^{-1}$ ), which played a minor role in characterizing structural transformations of DCE.

The samples were loaded at room temperature as liquid with nominal pressure slightly above ambient. Then the cell was carefully pressurized with small steps and allowed to stabilize for a few minutes after each pressure change before Raman spectra were taken. Pressure effects on DCE were examined both in the compression and decompression directions. Experiments were conducted up to 30 GPa and reproduced for a few times.

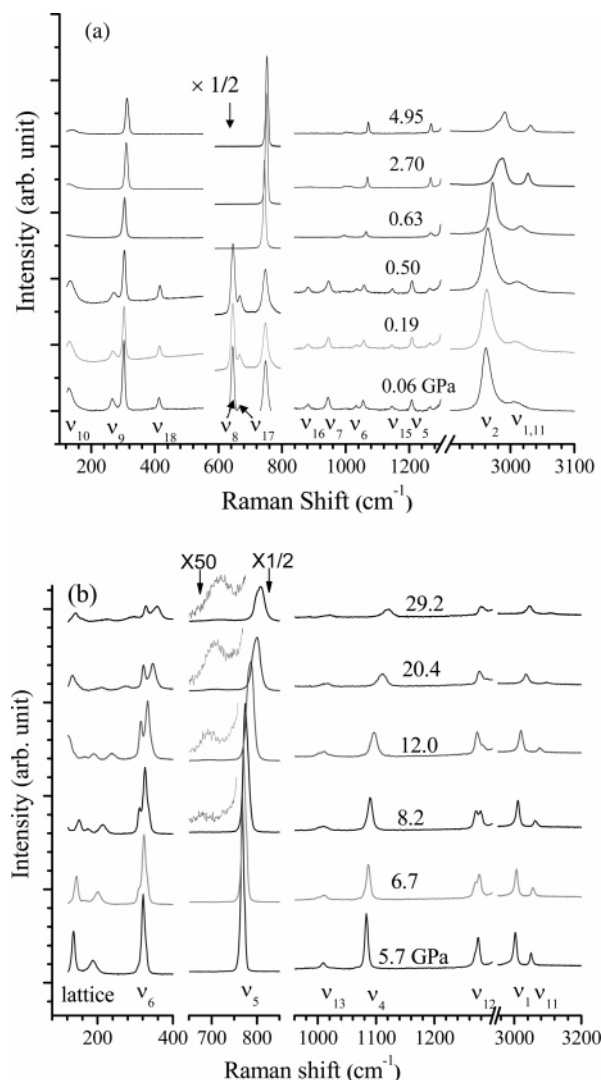


**Figure 2.** Selective Raman spectra of 1,2-dichloroethane on compression in the pressure region of (a) 0–5.0 and (b) 5.7–29.2 GPa in the spectral range of 120–1300 and 2900–3100 cm<sup>-1</sup>. The assignments of Raman active modes are labeled below for gauche (a) and trans (b) conformations. Due to the intense Raman modes of  $\nu_8$  and  $\nu_{17}$  for gauche and  $\nu_5$  for trans conformers, the spectra are rescaled by 1/2 of the original intensity in the spectral region of 600–800 cm<sup>-1</sup>. The Raman intensity in the spectral region of 650–750 cm<sup>-1</sup> above 8.2 GPa is zoomed 50 times in order to see the new mode (b). The relative intensities are normalized and thus are directly comparable. The pressures in GPa are labeled for each spectrum. The spectra are offset vertically for clarity.

### III. Results and Discussion

**A. Raman Spectra of DCE on Compression.** Raman spectra of DCE at selected pressures are depicted in Figure 2. The bottom spectrum of Figure 2a was obtained at near-ambient pressure corresponding to liquid phase. Room-temperature fluid DCE is composed of a mixture of trans and gauche conformers. As can be seen, all Raman active modes are observed at near-ambient pressure except for the region of strong diamond T<sub>2g</sub> mode, in excellent agreement with previous studies.<sup>4</sup> For clarity purposes, the Raman active modes only associated with gauche conformer are labeled in Figure 2(a) while those associated with the trans conformer are labeled in Figure 2(b). Of these modes,  $\nu_9$  and  $\nu_{18}$  at 263 and 412 cm<sup>-1</sup> (C–C–Cl bending) together with  $\nu_8$  and  $\nu_{17}$  at 655 and 674 cm<sup>-1</sup> (C–Cl stretching) are most distinctive as these modes involve chlorine atoms. Other modes

involving CH<sub>2</sub> motion, such as  $\nu_7$ ,  $\nu_{10}$ , and  $\nu_{13-16}$ , provide supplemental information about conformational equilibria. With increasing pressure up to 0.5 GPa, equilibrium is shifted from trans to gauche as evidenced by the increasing intensity of the  $\nu_8$  mode prominently with pressure (see Figure 6 for details). This observation is consistent with previous high-pressure Raman and IR study on DCE, in which Taniguchi et al.<sup>6</sup> showed that in solutions of hexane, 2-methylbutane and acetonitrile, the concentration of gauche conformer of DCE increases with pressure up to 0.5 GPa. The current study, however, indicates for the first time that the conformation equilibrium of pure DCE exhibits similar pressure effect. Quantitative analysis is discussed below.

When pressure is increased to 0.6 GPa, all the characteristic Raman modes associated with gauche conformer especially the prominent  $\nu_8$  and  $\nu_{17}$  C–Cl stretching mode suddenly disappeared, indicating DCE is in the trans conformation exclusively at this pressure. This abrupt change is in contrast with the trend of increasing gauche concentration with pressure below 0.5 GPa. We ascribe this discontinuity to the accompanied phase transition from fluid to solid. The observation of exclusive trans conformation in solid DCE induced by high pressure is consistent with previous low temperature study.<sup>3</sup> However, the pressure effect on pure DCE is in strong contrast to the previous Raman and infrared spectroscopic study on DCE in solutions at pressures up to 3.6 GPa. For example, Ikawa et al.<sup>7</sup> conducted room-temperature IR measurements of DCE with a concentration of 1.7% v/v in solutions of 2-methylbutane. Instead of transformation to 100% trans conformation as solid at 0.6 GPa, DCE remains soluble up to 3.6 GPa and is composed of both trans and gauche conformers. If pure DCE remains fluid at high pressures, the concentration of gauche conformer would have continued to increase with increasing pressure until it reaches 100%. Previous study indicated that dihedral angle of Cl–C–C–Cl changes at a rate of  $-0.2^\circ/\text{GPa}$ , at which the gauche conformation will become a strict cis (eclipsed) conformation at 1.5 GPa by extrapolation.<sup>6</sup> It would be therefore interesting to conduct a new experiment where pressurized pure DCE is maintained in a fluid phase all the time using a heated DAC to justify the extrapolation.

As DCE is further compressed beyond 0.6 GPa, all the nine Raman active modes of trans conformer exhibit pressure-induced shift to higher frequencies. At 5.7 GPa, prominent changes in the lattice region are observed. As shown in Figure 2(b), two new modes at 136 and 188 cm<sup>-1</sup> are suddenly resolved, although all internal vibration modes evolve smoothly with pressure. More lattice modes could have been observed below 120 cm<sup>-1</sup> if the cutoff spectral region of the edge filter were lower than that. The observation of sharp lattice modes indicates a transformation into a crystalline phase from a possible disordered structure or amorphous polymorph reported in a high-pressure X-ray diffraction measurement,<sup>9</sup> the nature of which is discussed below. More dramatic change of Raman patterns are observed at 8.2 GPa. Not only is a third lattice mode at 176 cm<sup>-1</sup> observed, but the  $\nu_6$  C–C–Cl bending mode around 325 cm<sup>-1</sup> starts to split into a doublet. Concurrently, the Raman peak of  $\nu_5$  C–Cl stretching mode is much weaker and broader. All these observations indicate the pressure-induced formation of a new phase. When pressure continues to increase all the way up to around 30 GPa, no further prominent changes in the Raman pattern are observed except the intensity is weaker.

**B. Raman Spectra of DCE on Decompression.** Reversibility of the pressure effect on structural transformation provides important information about the transformation mechanism.

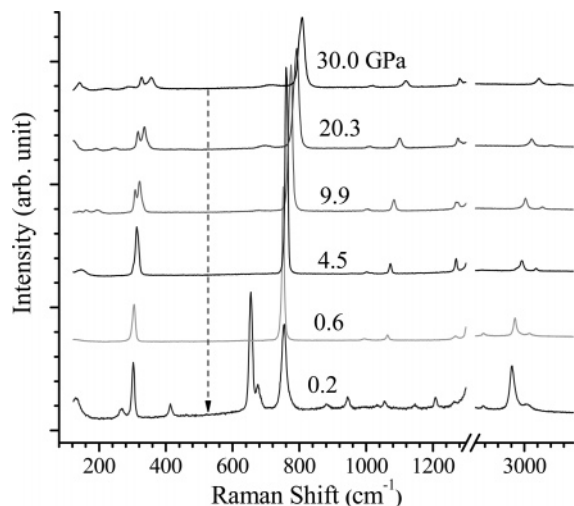


**Figure 3.** Selective Raman spectra of 1,2-dichloroethane on decompression from around 30 GPa all the way down to ambient pressure. Due to the intense  $T_{2g}$  Raman mode of diamond anvils, the spectra were truncated above  $1300\text{ cm}^{-1}$ . The spectra are offset vertically for clarity. The relative intensities are normalized and thus are directly comparable. The dashed arrow indicates the experimental sequence for decompression.

Therefore, we investigated the reversibility of the pressure induced transformations of DCE in the entire pressure region. Figure 3 depicts the Raman spectra of DCE on decompression from the highest pressure of 29.2 GPa all the way down to near ambient pressure. Opposite to compression, all the Raman frequencies shift to low energies. As a result, the prominent lattice mode at  $142\text{ cm}^{-1}$  at 29.2 GPa shifts to outside the detectable region below  $120\text{ cm}^{-1}$  below 20.3 GPa due to the use of an edge filter. All the other Raman modes exhibit reversible pressure responses on decompression all the way down to 0.6 GPa, including the appearance of the lattice modes, merging of the doublet of  $\nu_6$  C–C–Cl bending mode, as well as the narrowing of all peak widths and enhanced peak heights. When the pressure is further released from 0.6 to 0.2 GPa, new Raman active modes associated with gauche conformation of DCE are observed, indicating the transformation between trans and gauche conformation is completely reversible. The decompression experiment was repeated starting from different highest pressures and all yielded reproducible phase transformations consistent with those upon compression.

**C. Pressure Effect on Raman Modes of DCE.** Figure 4 depicts the Raman shifts as a function of pressure on compression from near ambient pressure up to around 30 GPa in the spectral range of both lattice and internal vibrational regions. Out of nine Raman active vibrational modes, seven are plotted except the  $\nu_3$  ( $\text{CH}_2$  wagging) and  $\nu_2$  ( $\text{CH}_2$  bending) modes which overlap with  $T_{2g}$  mode of diamond. The pressure dependence of these modes is listed in Table 2. As can be seen, no appreciable pressure induced frequency shift is observed for any Raman mode in the low-pressure region of 0–0.5 GPa. Therefore, pressure only affects the equilibrium between gauche and trans conformers in the fluid DCE. All Raman active modes exhibit significant pressure-induced shift to higher frequencies when DCE becomes solid above 0.6 GPa, but to different extent which provides critical information about phase transformations. In the high-frequency region, both the antisymmetric ( $\nu_{11}$ ) and symmetric ( $\nu_1$ ) C–H stretching modes ( $3003$  and  $2959\text{ cm}^{-1}$  respectively at ambient pressures) display distinctively different rates around 8–9 GPa. Below the transition pressure, large pressure shift rates of  $8.7$  and  $6.0\text{ cm}^{-1}/\text{GPa}$  are observed for

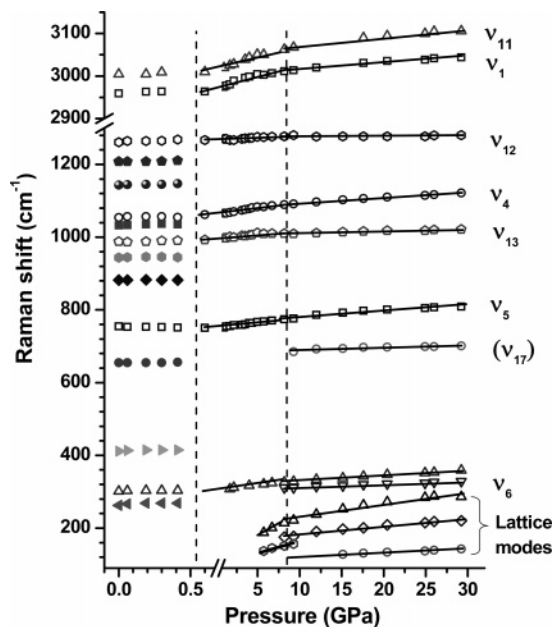


**Figure 4.** Raman shift of 1,2-dichloroethane with pressure on compression. Different symbols denote Raman modes with different origins. Open and closed symbols denote trans and gauche conformers of 1,2-dichloroethane respectively. The solid lines crossing the open symbols are for eye guidance. The vertical dashed lines denote proposed phase boundaries. The transition at about 5 GPa is not labeled. The assignments are labeled for each Raman active mode. The  $\nu_{17}$  mode is parenthesized because it is not a Raman active mode under trans symmetry (see text).

**TABLE 2: Pressure Dependence of Raman Shifts of 1,2-Dichloroethane**

Raman mode	frequency at ambient-P ( $\text{cm}^{-1}$ )	$(d\nu/dP)_T$ ( $\text{cm}^{-1}/\text{GPa}$ )	
		0.5–8 GPa	9–30 GPa
$\nu_{11}$	3003	8.7	2.3
$\nu_1$	2959	6.0	1.7
$\nu_{12}$	1261	2.6	0.2
$\nu_4$	1054	3.7	1.6
$\nu_{13}$	988	2.4	0.5
$\nu_{17}^a$	684		0.5
$\nu_5$	755	3.2	1.7
$\nu_6$	302	3.8	1.3
lattice modes		13.4	3.2
			2.1
		11.7	5.2
			0.9

<sup>a</sup> A new mode at  $692\text{ cm}^{-1}$  with very weak intensity was observed starting 9 GPa on compression. If extrapolated to ambient pressure, this mode ( $684\text{ cm}^{-1}$ ) is in the close vicinity of  $\nu_{17}$  mode ( $677\text{ cm}^{-1}$ ) for the gauche conformer.

these two modes while the rates become much smaller ( $2.3$  and  $1.7\text{ cm}^{-1}/\text{GPa}$ , respectively) above 9 GPa. In contrast, the  $\nu_{12}$  ( $\text{CH}_2$  twisting) mode exhibits very small pressure rate of only  $1.2\text{ cm}^{-1}/\text{GPa}$  below 8 GPa, and no appreciable pressure induced shift is observed in a broad pressure region of 9–30 GPa. Other modes, such as  $\nu_4$  (C–C stretching),  $\nu_{13}$  ( $\text{CH}_2$  rocking), and  $\nu_5$  (C–Cl stretching) all exhibit a distinctive change of pressure dependence at 8–9 GPa again. An intriguing observation is that a Raman mode at  $684\text{ cm}^{-1}$  becomes significantly enhanced at 8.18 GPa as shown in the zoomed spectra (Figure 2b). The change of Raman intensities provides additional evidence for a possible pressure-induced phase transformation as a result of

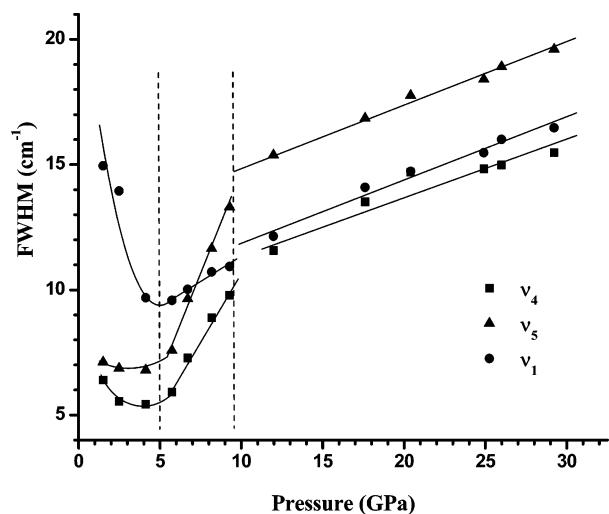


**Figure 5.** Full-width-at-half-maximum (fwhm) of three representative Raman modes ( $\nu_1$ ,  $\nu_5$ , and  $\nu_4$ ) as a function of pressure for solid phases of 1,2-dichloroethane. The solid curves and lines across the symbols are for eye guidance. The dashed line denotes the proposed phase boundaries.

increasing vibrational coupling. As a non-Raman active mode for trans geometry, this mode may have similar origin to the  $\nu_{17}$  (C–Cl stretching) mode of both trans and gauche conformers (709 and 677  $\text{cm}^{-1}$ ). The most prominent change is observed for the  $\nu_6$  (C–C–Cl bending) mode which exhibits a striking splitting above 8.2 GPa. All these features clearly indicate a phase transformation around this pressure, which are discussed in detail next.

Transformation can be further evidenced by the pressure behavior of lattice modes. Previous low- $T$  Raman study of solid DCE revealed that all lattice modes are below 120  $\text{cm}^{-1}$ , the detection limit of the current Raman spectrometer due to the use of an edge filter. Nonetheless, as pressure will typically induce blue shift, these lattice modes will be observed at higher frequencies upon compression if they exist. Then by extrapolation to ambient pressure, the lattice modes can be identified with assignment if they evolve from lattice structures at low-temperature and ambient pressure. However, the extrapolated values of these modes give near zero or negative values using either linear or quadratic functions, indicating these modes have completely different origins than the previously reported values of 117, 79, 73 and 55  $\text{cm}^{-1}$ , which were assigned as the rotatory lattice vibrations. The observation of these new lattice modes indicates that the crystal structure at high pressures and room temperature is different than that at the ambient pressure and low-temperature conditions. Further, these lattice modes provide consistent information about phase transformations at around 8–9 GPa, similar to the internal vibrational modes.

Pressure induced transformations are observed in many molecular crystals. An important piece of information to understand the structures of each of the new phases formed at high pressures can be obtained from the widths of the characteristic peaks. Figure 5 depicts the widths of selected Raman modes as a function of pressure in the region of 0.5 to 30 GPa.  $\nu_1$  ( $\text{CH}_2$  symmetric stretching),  $\nu_4$  (C–C stretching) and  $\nu_5$  (C–Cl stretching), which were observed at 2959, 1054 and 755  $\text{cm}^{-1}$  at ambient pressure, are selected because these modes exhibit the most prominent pressure-induced width broadening. Interestingly, these modes display turn-around behavior with pressure, i.e., their width first decrease until around 5 GPa, then increase until about 9 GPa. All the three modes exhibit a sudden increase in peak width at that pressure

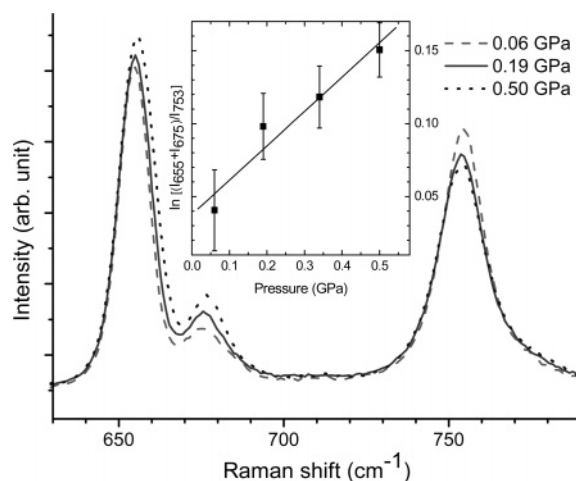


**Figure 6.** Selective Raman spectra of 1,2-dichloroethane in the zoomed spectra region of 600–800  $\text{cm}^{-1}$  in fluid phase. The inset is the plot of logarithm of relative intensities of the first two peaks over the third peak as a function of pressure (see text).

and continue to 30 GPa almost linearly. These changes provide further evidence of phase transformations at 4–5 GPa and 8–9 GPa, highly consistent with those determined by examining the shift rate of Raman frequency with pressure. Although all vibrational modes in the entire pressure region between 0.6 and 8.2 GPa exhibits a smooth evolution, the pressure dependence of peak widths provides unambiguous evidence for the first transition at 4–5 GPa.

#### D. Discussion

Raman measurements at low pressures (<0.5 GPa) yielded consistent information of pressure effect on trans–gauche equilibrium of DCE with previous Raman and IR studies of DCE in different solvents.<sup>6,7</sup> Quantitative analysis of relative Raman intensities characteristic of two conformers showed that DCE exhibits both solvent- and concentration-dependent transformation volumes from trans to gauche. Accordingly, similar analysis can be carried out in this first study on pure DCE at high pressures. Figure 6 shows the selective zoomed Raman spectra in the spectral region of 620–800  $\text{cm}^{-1}$  where three characteristic peaks associated with two conformers (655 and 675  $\text{cm}^{-1}$  for gauche and 765  $\text{cm}^{-1}$  for trans) are observed. Clearly, with increasing pressure, the relative intensity of gauche versus trans increased markedly, indicating the equilibrium is shifted to gauche. The transformation volume can be calculated via the equilibrium constant using the following relationship:<sup>6</sup>

$$\left(\frac{\partial \ln K}{\partial P}\right)_T = -\frac{\Delta V}{RT} \quad (1)$$

where  $K$  is the equilibrium constant, which can be calculated as  $(I_{655} + I_{675})/I_{765}$ , with  $I_\omega$  being the peak intensity at the given frequency  $\omega$ ,  $\Delta V$  the transformation volume,  $R$  the gas constant, and  $P$  and  $T$  the pressure and temperature. From the inset of Figure 6, linear regression of  $\ln K$  versus pressure at room temperature yields the transformation volume of  $0.58 \pm 0.10 \text{ cm}^3/\text{mol}$ . This value is significantly smaller than those for the DCE in different solvents with different concentrations determined in previous studies, ranging from 1.8 to 4.5  $\text{cm}^3/\text{mol}$ ,<sup>6</sup> but is consistent with that reported by McClain<sup>14</sup> ( $\sim 1 \text{ \AA}^3$  or 0.6  $\text{cm}^3/\text{mol}$ ). These observations confirm that properties of solvent significantly altered the transformation volume between two conformers, while the difference in intrinsic volumes of the two

conformers is much smaller in pure fluid DCE and is strongly modulated by pressures.

Solid DCE revealed intriguing pressure behavior which enables the identification of three new phases at 0.6–30 GPa based on the above analysis. Previous single-crystal X-ray diffraction also identified two phases at ambient pressure and low temperatures, which were labeled ordered  $\beta$  phase (<177 K) and disordered  $\alpha$  phase (177–238 K).<sup>15,16,19</sup> The primary difference between the two phases is that the  $-\text{CH}_2-$  groups showing near free rotations or orientational disorder approximately along the Cl–C–C–Cl axis at higher temperature become completely frozen and thus ordered in the low-temperature phase. More recently, a high-pressure X-ray diffraction study of single-crystal DCE by Bujak et al.<sup>9</sup> indicated that the low-temperature phases are correlated with high-pressure phases. The crystal structure of DCE was refined at 0.7 GPa and near room temperature, which yielded consistent parameters with the disordered structure of  $\alpha$ -phase. It was found that the disorder involves the ethylene group ( $-\text{CH}_2-\text{CH}_2-$ ) in two sites with equal occupancies, such that one rotated by  $180^\circ$  to the other along the primary Cl...Cl axis. The comparison of the high-pressure  $\alpha$ -phase and low-temperature  $\beta$ -phase suggests that order–disorder transition is governed by the competition of the nonbonding Cl–Cl interactions with the ethylene rotations. Although it was further found DCE may form a new polymorph with a possible amorphous structure when compressed to about 1.5 GPa due to the non-homogeneous strain, the current Raman measurements do not show corresponding spectroscopic features that allows the identification of a sharp phase boundary at this pressure. Nonetheless, the lack of sharp lattice modes together with the broad profile of  $\nu_{13}$  ( $\text{CH}_2$  rocking) and  $\nu_1$  (C–H symmetric stretching) modes at pressures between 0.5 and 5 GPa is consistent with a disordered or amorphous phase. The nature of this phase can be considered as a transitional region that connects two crystalline phases. Therefore, the current Raman measurements, when combined with previous Raman and the single-crystal X-ray diffraction study, indicate the amorphous polymorph may be extended to around 5 GPa.

At around 5 GPa, the DCE undergoes an intriguing opposite transformation, i.e., from a possible amorphous polymorph to a crystalline phase as evidenced by the appearance of two sharp rotatory lattice modes at 136 and 188  $\text{cm}^{-1}$ . Furthermore, the peak widths of three representative vibrational modes ( $\nu_1$ ,  $\nu_5$ , and  $\nu_4$ ) all exhibit pressure induced narrowing. These features indicate that DCE is transforming into a crystalline phase with most ordered structure at round 5 GPa (Figure 5). In the disordered  $\alpha$ -phase, the shortest intermolecular distance between chlorine atoms is 3.587 Å, significantly longer than that in the ordered  $\beta$ -phase (3.387 Å). This distance in  $\beta$ -phase is also significantly shorter than the sum of van der Waals radii of Cl atoms, suggesting that specific interactions exist between DCE molecules plays a critical role in packing mode and molecular association to form the ordered crystalline phase. Since pressure can significantly reduce the intermolecular distance, it is therefore plausible to conclude that the pressure is high enough to bring neighboring DCE molecules close to each other at about 5 GPa, such that the intermolecular Cl–Cl distance becomes comparable with that in the ordered  $\beta$ -phase. Under such conditions, the free rotation of  $-\text{CH}_2-$  group is suppressed by high pressure. The pressure-induced ordering as a result of freeze of rotation has been observed in other systems. For example, high pressure study of nitrosonium nitrate ( $\text{NONO}_3$ ) indicates that the NO group is freely rotating at low pressures but the

structure becomes ordered at high pressures.<sup>11</sup> On the basis of the spectroscopic measurements where no abrupt changes were observed upon compression, the structure of this ordered phase of DCE may be similar to those of  $\alpha$ - and  $\beta$ -phases to remain a monoclinic  $P2_1/c$  symmetry. However, as the lattice modes of the current phase do not correspond to the low-temperature  $\beta$ -phase, detailed atomic orientations may be different, which could even result in a different (sub)space group. Of course, unambiguous interpretation of the ordered structure would require X-ray diffraction measurement.

Between 5 and 8 GPa, smooth evolution of all Raman active modes with pressure indicates a single ordered phase of DCE in this pressure region. Beyond 9 GPa, significant changes in the slopes of Raman shifts versus pressure (Figure 4) as well as the abrupt changes of the peak widths of  $\nu_1$ ,  $\nu_5$ , and  $\nu_4$  modes (Figure 5) indicate a phase transition. Starting from this pressure, not only all the lattice modes become much weaker, but all the external vibrational modes exhibit a significant peak broadening. Two prominent new features signify the formation of a new phase: (1) the splitting of the  $\nu_6$  mode and (2) the appearance of a new mode at 692  $\text{cm}^{-1}$  (Figure 2b, Figure 4 and Table 2), a non-Raman active mode for the trans conformer. All these observations suggest the stronger interactions among DCE due to the shorter intermolecular distance upon compression. The origin of splitting of Raman modes is highly likely associated with correlation field effect due to the pressure induced dipole–dipole interaction of neighboring molecules within the unit cell. As a result, the molecular symmetry or the cell symmetry is lowered such that new Raman modes are now active and observed. The pressure induced lower symmetry with peak splittings and appearance of new peaks has been observed in other simple molecular crystals before.<sup>13</sup>

In contrast to solid phases below 8 GPa, the changes of the Raman patterns with pressure above 9 GPa is more gradual. Less steep shift rates are observed for most Raman modes including both the vibrational and the lattice modes (Figure 4 and Table 2). Furthermore, abrupt changes of peak widths versus pressure of the three selected Raman modes to much less steep are observed at 9 GPa. The change of slopes of Raman shifts versus pressure as well as peak widths indicates the solid DCE at above 9 GPa is less compressible than below. In this pressure region, intensities of all the Raman modes are significantly depleted. In addition, the bandwidths of major Raman modes, such as  $\nu_5$  (C–Cl stretching) and  $\nu_{13}$  ( $\text{CH}_2$  rocking), exhibit substantial broadening. More significantly, no sharp lattice feature but only one broad band can be observed all the way to 29 GPa. Peak broadening could be due to pressure gradient with increasing pressures especially when no pressure media were used. However, the reasonably well separated  $R_1$  and  $R_2$  lines of ruby fluorescence at the highest pressure together with multiple measurements on different areas of the sample indicate pressure gradient played a minor role in peak broadening. Furthermore, the decompression experiments established that all pressure-induced transformations in DCE are entirely reversible. The recovered Raman spectra indicate that DCE maintains its chemical identity even at highest pressures which rules out pressure-induced decomposition. All these observations indicate that with increasing pressure, the ordered crystalline structure may undergo a gradual transformation with increasing degree of disorder and likely, an amorphization. Again, the detailed pressure-induced structural information needs to be confirmed by X-ray diffraction.

Conformational and phase transformations of all halogen substituted ethane are of fundamental interests and have been

extensively studied by Raman, IR spectroscopy and theoretical calculations.<sup>20–22</sup> The study of structures of DCE in the context with other halogen substituted 1,2-dihalogenethane(DHE) therefore provides important insight in the systematic understanding of structures and transformations of all DHE. In fluid phase, all the DHE exist as a mixture of trans and gauche conformers, but with different relative abundance. From 1,2-difluoroethane (DFE) to 1,2-diiodoethane (DIE), the gauche to trans ratio decreases from 96%:4% to 12%:88% at ambient conditions. Solid DFE crystallizes into two phases both with gauche conformation. The first phase formed at 158 K is monoclinic  $C2/c$  while second phase formed at slight lower temperature (128 K) has an orthorhombic space group  $P2_12_12_1$ , both with four molecules per cell and F–C–C–F dihedral angle close to 68°.<sup>23</sup> Apparently, the ambient structure of DCE is significantly different than DFE for which the high-pressure phases are still totally unexplored yet. In contrast, DIE crystallizes in a similar unit cell to DCE with only a slightly different monoclinic space group of  $P2_1/n$ .<sup>23</sup> In this structure, the two neighboring iodine atoms with short distances are strongly interacted to form an ordered structure similar to the low-temperature  $\beta$ -phase of DCE.

In addition to the current study of DCE, other DHE that have been studied at high pressures include only 1,2-dibromoethane (DBE). Shimizu et al.<sup>22</sup> have measured Raman patterns of DBE up to 12 GPa at room temperature. With exactly the same Raman active modes, high-pressure behavior of DBE is highly similar to DCE in both the fluid and solid phases in terms of trans–gauche equilibrium and phase transformations, except the transformation pressures are different. For example, liquid-to-solid transition of DBE occurs at 0.1 GPa, much lower than that for DCE. The pressure evolution of characteristic Raman modes of DBE, such as  $\nu_6$  (C–C–Br bending),  $\nu_5$  (C–Br stretching),  $\nu_4$  (C–C stretching),  $\nu_3$  (CH<sub>2</sub> wagging) and  $\nu_1$  and  $\nu_{11}$  (symmetric and antisymmetric CH stretching), all exhibit a significant change of pressure rate indicates a phase transformation at 6.3 GPa, similar to that observed in DCE at 8.2 GPa. In addition, the  $\nu_5$  and  $\nu_6$  modes splitted into doublet above the transition pressure, in analogy to the splitting of  $\nu_6$  mode of DCE. All these observations indicate the phase transformations for DBE at 6.3 GPa and that for DCE at 8.18 GPa have a similar nature. Although the ambient pressure crystal structure of DBE is not known yet, it is plausible to interpolate its structure to be highly likely monoclinic based on the structures of DCE and DIE.

Although current studied yield rich new information of the high-pressure structures of DCE, its exact structures need to be confirmed by X-ray diffraction. Furthermore, the study of DCE, if extended to both high and low temperatures, will yield complete picture of its phase diagram. Similar studies should also be extended to other DHE, such as DFE and DIE. All these work are planned in the near future.

#### IV. Conclusions

We investigated the behavior of 1,2-dichloroethane at high pressures up to 30 GPa at room temperature using Raman spectroscopy. In the low-pressure range of 0–0.5 GPa, DCE exists as a mixture of gauche and trans conformers in the fluid phase. Compression results in the shift of the equilibrium from trans to gauche with transformation volume of  $0.58 \pm 0.10 \text{ cm}^3/\text{mol}$ , indicating the intrinsic volume change of pure DCE is smaller than in different solvents reported previously. At 0.6 GPa, DCE experiences a phase transformation from fluid to solid in which only trans conformation of DCE is observed, consistent with previous study at low-temperature and ambient pressure.

The low-pressure solid DCE is likely a disordered or amorphous phase due to the lack of lattice vibrations, consistent with previous study by single-crystal X-ray diffraction. When DCE is further compressed, it becomes ordered crystalline phase characterized by new lattice modes at 5 GPa. Beyond 9 GPa, DCE exhibits a phase transformation evidenced by the splitting of degenerate Raman modes as well as new lattice mode. The high-pressure phase is likely a crystalline phase but with lower symmetry than the low-pressure phase. This phase becomes more disordered with significant peak broadening when further compressed up to 30 GPa. Both pressure-induced conformational and phase transformations are completely reversible upon decompression. The structures of DCE are examined in comparison with other halogen substituted ethane. Further spectroscopic and X-ray diffraction measurements are necessary to yield unambiguous structural information for DCE at high pressures.

**Acknowledgment.** The authors are grateful for M.J. Walzak at Surface Science Western for her assistance with the Raman instrumentation. This work is supported by the research grants from Natural Sciences and Engineering Research Council of Canada and Academic Development Fund from the University of Western Ontario.

#### References and Notes

- (1) Hemley, R. J. *Annu. Rev. Phys. Chem.* **2000**, *51*, 763.
- (2) Song, Y.; Hemley, R. J.; Mao, H. K.; Herschbach, D. R. In *Chemistry under Extreme Conditions*; Manaa, M. R., Ed.; Elsevier: Amsterdam, 2005; pp 189.
- (3) Nakagawa, I.; Mizushima, S. *J. Chem. Phys.* **1953**, *21*, 2195.
- (4) Mizushima, S.; Shimanouchi, T.; Harada, I.; Abe, Y.; Takeuchi, H. *Can. J. Phys.* **1975**, *53*, 2085.
- (5) Takaya, H.; Taniguchi, Y.; Wong, P. T. T.; Whalley, E. *J. Chem. Phys.* **1981**, *75*, 4823.
- (6) Taniguchi, Y.; Takaya, H.; Wong, P. T. T.; Whalley, E. *J. Chem. Phys.* **1981**, *75*, 4815.
- (7) Ikawa, S.; Whalley, E. *J. Chem. Phys.* **1984**, *81*, 1620.
- (8) Georgieva, G.; Dudev, T.; Galabov, B.; Durig, J. R. *Vib. Spectrosc.* **1992**, *3*, 9.
- (9) Bujak, M.; Budzianowski, A.; Katrusiak, A. *Z. Kristall.* **2004**, *219*, 573.
- (10) Hemley, R. J.; Mao, H. K. In *High-Pressure Phenomena, Proceedings of the International School of Physics Enrico Fermi*; Hemley, R. J., Chiarotti, G. L., Bernasconi, M., Ulivi, L., Eds.; IOS Press: Amsterdam, 2002; Vol. 147, p 3.
- (11) Song, Y.; Hemley, R. J.; Liu, Z. X.; Somayazulu, M.; Mao, H. K.; Herschbach, D. R. *J. Chem. Phys.* **2003**, *119*, 2232.
- (12) Song, Y.; Hemley, R. J.; Mao, H. K. A.; Liu, Z. X.; Herschbach, D. R. *Chem. Phys. Lett.* **2003**, *382*, 686.
- (13) Song, Y.; Liu, Z. X.; Mao, H. K.; Hemley, R. J.; Herschbach, D. R. *J. Chem. Phys.* **2005**, *122*, 174511.
- (14) McClain, B. L.; Ben-Amotz, D. *J. Phys. Chem. B* **2002**, *106*, 7882.
- (15) Milberg, M. E.; Lipscomb, W. N. *Acta Crystallogr.* **1951**, *4*, 369.
- (16) Reed, T. B.; Lipscomb, W. N. *Acta Crystallogr.* **1953**, *6*, 45.
- (17) Boese, R.; Blaser, D.; Haumann, T. *Z. Kristallogr.* **1992**, *198*, 311.
- (18) Mao, H. K.; Xu, J.; Bell, P. M. *J. Geophys. Res.* **1986**, *91*, 4673.
- (19) Lipscomb, W. N.; Wang, F. E.; May, W. R.; Lippert, E. L. *Acta Crystallogr.* **1961**, *14*, 1100.
- (20) Goodman, L.; Gu, H. B.; Pophristic, V. *J. Phys. Chem. A* **2005**, *109*, 1223.
- (21) Durig, J. R.; Liu, J.; Little, T. S.; Kalasinsky, V. F. *J. Phys. Chem.* **1992**, *96*, 8224.
- (22) Shimizu, H.; Miyahara, N. *Chem. Phys. Lett.* **1984**, *110*, 615.
- (23) Akkerman, F.; Buschmann, J.; Lentz, D.; Luger, P.; Rodel, E. *J. Chem. Crystallogr.* **2003**, *33*, 969.